Neuroscience Letters 753 (2021) 135846

Contents lists available at ScienceDirect

Neuroscience Letters

journal homepage: www.elsevier.com/locate/neulet

Research article

Persistent sodium conductance contributes to orexin-A-mediated modulation of membrane excitability in neonatal rat mesencephalic V neurons

Susumu Tanaka [a,*], Soju Seki [a], Yudai Ono [a], Akifumi Enomoto [b], Mikihiko Kogo [a]

[a] First Department of Oral and Maxillofacial Surgery, Graduate School of Dentistry, Osaka University, 1-8 Yamadaoka, Suita, Osaka, 565-0871, Japan
[b] Department of Oral and Maxillofacial Surgery, Faculty of Medicine, Kindai University, 377-2 Ohno-higashi, Osaka-Sayama, 589-8511, Japan

ARTICLE INFO

Keywords:
Mesencephalic trigeminal neuron
Orexin
Oral motor activity
Patch clamp
Sensory neurons

ABSTRACT

Orexins are multifunctional hypothalamic neuropeptides that participate in the stimulation of feeding behavior and energy expenditure. However, little is known about their neuromodulatory effects in lower brainstem effector regions, including in the trigeminal neuronal system. The aim of this study was to examine the effects of orexin-A (Ox-A) on the membrane properties of mesencephalic trigeminal (Mes V) neurons that are critically involved in the generation and control of rhythmical oral motor activities. Whole-cell patch clamp recordings were obtained from Mes V neurons in coronal brain slices prepared from Sprague-Dawley rats (postnatal day 12–17). Bath application of Ox-A (100 nM) shortened the duration of the after-hyperpolarization following the action potential, while the interspike frequency of firings during repetitive discharge increased, together with a shift in the frequency-current relationship toward the left. In addition, Ox-A amplified the resonance at the depolarized membrane potential, accompanied with an increase in both Q-value and resonant frequency. A further voltage-clamp experiment demonstrated that Ox-A increased the peak current density of the persistent sodium current (I_{NaP}) and shifted its activation curve to the hyperpolarization direction. These results suggested that Ox-A may increase Mes V neuronal excitability by enhancing I_{NaP}, possibly sharing a common mechanism with another orexigenic hypothalamic neuropeptide, neuropeptide Y.

1. Introduction

The hypothalamic neurons synthesize and release various types of neuropeptide, which are believed to project throughout the brain and regulate behavior related to energy homeostasis. Orexins, consisting of orexin-A (Ox-A) and orexin-B (Ox-B) isoforms, are hypothalamic neuropeptides produced by a small number of neurons in the lateral and posterior hypothalamic areas [1]. These orexinergic neurons project throughout the brain, including to the lower brainstem regions [2], and regulate various homeostatic processes including the sleep-wake cycle, energy expenditure, and modulation of visceral functions [1]. Furthermore, the orexinergic system is critically involved in analgesia and in behaviors associated with morphine withdrawal, and has recently been suggested to regulate nociceptive function and arousal state through shared neural circuits [3,4].

Regarding motor control, orexin exhibits powerful orexigenic effects and is believed to contribute to the regulation of feeding behavior [1]. Supporting this, intracerebroventricular injection of orexin shortens the latency to begin feeding and increases the total amount of food intake in rats [5,6]. Furthermore, Ox-A exhibits more potent effects than Ox-B in facilitative responses in feeding behavior, and amplifies the electromyographic activities of masticatory muscles [6].

Immunohistochemical studies have revealed that orexigenic neurons directly project into trigeminal motoneurons, which specifically express orexin receptors [2,7]. Interestingly, microinjection of orexins into the trigeminal motor nucleus in a decerebrate cat preparation substantially increases masseter muscle tone, suggesting that orexins can directly affect motoneurons [8]. Supporting these results, Ox-A depolarizes the membrane and induces inward current, accompanied by an increased action potential peak amplitude and interspike frequency of bursting activities, thus increasing membrane excitability in trigeminal motoneurons [9].

Trigeminal motoneurons integrate central synaptic inputs from surrounding neurons, including mesencephalic trigeminal (Mes V) neurons

* Corresponding author.
E-mail address: stanaka@dent.osaka-u.ac.jp (S. Tanaka).

https://doi.org/10.1016/j.neulet.2021.135846
Received 15 September 2020; Received in revised form 10 January 2021; Accepted 22 March 2021
Available online 24 March 2021

and other premotor neurons. Mes V neurons are sensory neurons with peripheral innervation of jaw-closer muscle spindles and central projections to various regions, including trigeminal interneurons and motor neurons. Mes V neurons have capability of the production of subthreshold oscillation, resonance, and intrinsic bursting activity [10–12], and neuropeptide Y (NPY), another orexigenic neuropeptide produced by the hypothalamic arcuate nucleus, could effectively modulate these properties with increased neuronal excitability [13]. While previous studies have revealed the projection of orexin-immunoreactive fibers and the expression of specific orexin in Mes V neurons [14,15], whether orexin affects Mes V neuronal excitability remains unclear.

Based on these findings, we suggest that Ox-A could also modulate

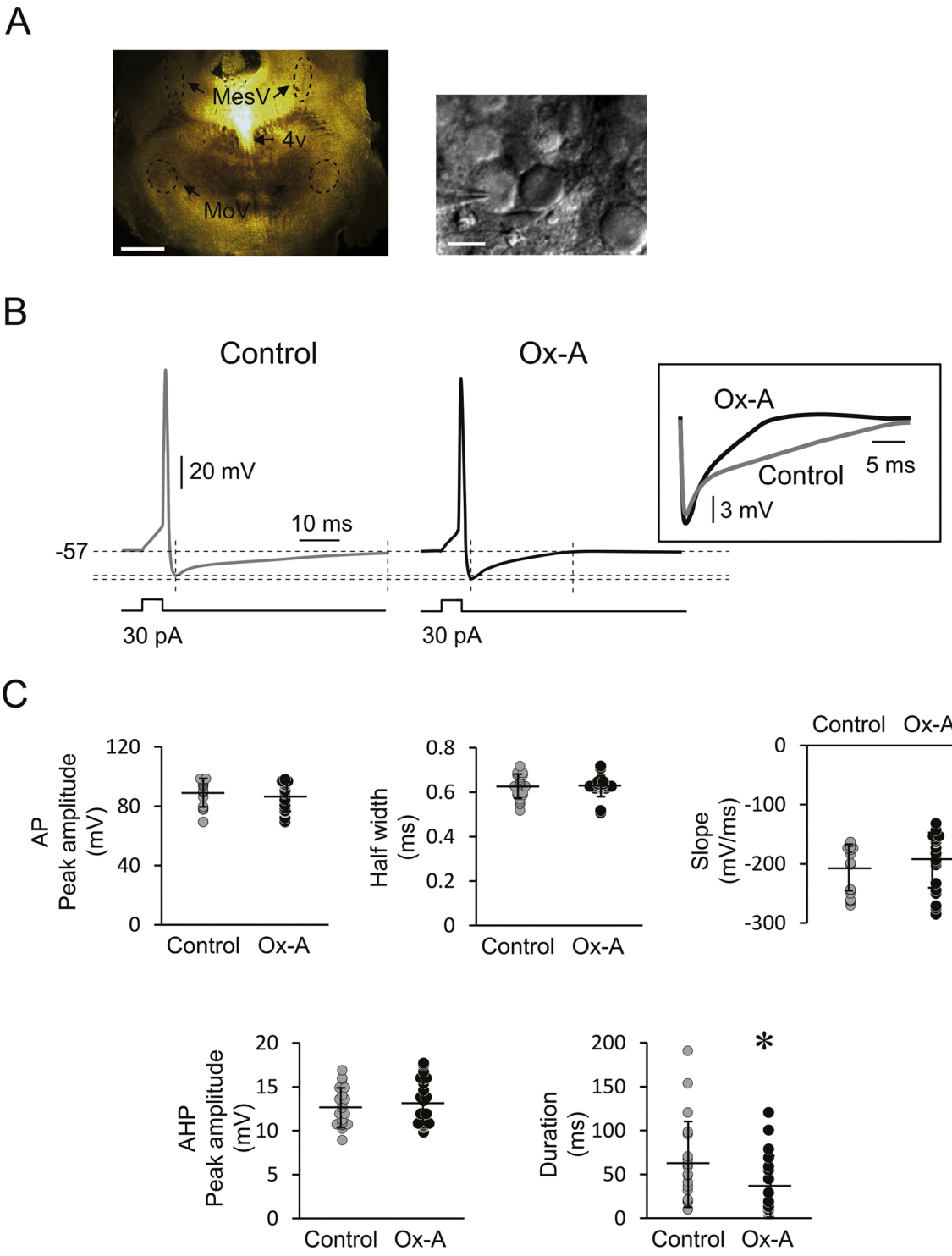

Fig. 1. Effects of orexin A (Ox-A) on action potential properties in Mes V neurons.
A: Histological verification of the recording site in large (left) and fine (right) scale focused on the whole-cell configuration. Mes V, mesencephalic trigeminal nucleus; MoV, trigeminal motor nucleus; 4 V, fourth ventricle. Scale bar: 1 mm (left), 30 μm (right). B: Representative voltage responses evoked by a short (3 ms) depolarizing step pulse before and after application of Ox-A in postnatal day 12 (P12) neurons. C: Ox-A did not alter the action potential properties, including spike height and half width, but did modestly increase peak amplitude and significantly shorten AHP duration. *$P <$ 0.05.

the membrane excitability of Mes V neurons. Therefore, in the present study, using the whole-cell patch clamp recording technique, we investigated the modulatory effects of Ox-A on the spike discharge characteristics and resonant behaviors of Mes V neurons.

2. Material and methods

2.1. Animals and brain slice preparation

All experiments were conducted in accordance with the guidelines for the Proper Conduct of Animal Experiments established by the ARRIVE guidelines, the Animals (Scientific Procedures) Act 1986, Directive 2010/63/EU for animal experiments, and were approved by the Osaka University Graduate School of Dentistry, Department of Animal Care and Use Committee (Doha-20−005-0). Sprague-Dawley rats (postnatal day 12–17, P12–17) were used. After birth, neonatal rat pups (the sex of pups was not determined, n = 35) were housed with the mother rat for breastfeeding under a 12-h/12-h light/dark cycle at a constant temperature of 21 ± 1 °C with 40 %–80 % humidity. Rats were anesthetized by halothane inhalation, and the brainstems were carefully removed and immersed in oxygenated ice-cold cutting solution (126 mM NaCl, 3 mM KCl, 1.25 mM NaH_2PO_4, 26 mM $NaHCO_3$, 10 mM glucose, 1 mM $CaCl_2$, 5 mM $MgCl_2$, and 4 mM lactic acid). Coronal brain slices containing the mesencephalic trigeminal nucleus (thickness, 300 μm) were prepared with a microslicer (Linear slicer PRO 7, Dosaka EM Co., Ltd., Kyoto, Japan) and incubated for 40 min at 37 °C before recordings began. The recording solution (normal artificial cerebrospinal fluid, ACSF) contained 124 mM NaCl, 3 mM KCl, 1.25 mM NaH_2PO_4, 26 mM $NaHCO_3$, 10 mM glucose, 2 mM $CaCl_2$, and 2 mM $MgCl_2$. All solutions were equilibrated with 95 % O_2, 5% CO_2, and the pH was adjusted to 7.3 (22–24 ℃).

2.2. Patch-clamp recordings and data analysis

Mes V neurons were visually identified by their pseudounipolar somata and located bilaterally and dorsally as an ellipsoid region under low magnification (5X) in each brain slice (Fig. 1A) [10–12]. Mes V neurons were secured in an acrylic recording chamber on the stage of an upright Nomarski infrared differential interference microscope (BX51W1, Olympus Optical Co., Ltd). Neurons with multipolar dendritic processes were excluded from the recordings. Whole-cell recordings from Mes V neurons were obtained throughout the rostral-caudal extent of the nucleus to avoid sampling bias (66 neurons from 48 coronal slices) using a Multiclamp 700B patch-clamp amplifier and pCLAMP acquisition software (Axon Instruments, Foster City, CA, USA). Thick-walled borosilicate fire-polished glass (OD, 1.5 mm; ID, 0.86 mm) and fabricated recording patch electrodes (tip resistance, 3.0–5.0 MΩ) with a programmable puller (Sutter Instruments P-97, Novato, CA, USA) were used. The composition of the intrapipette solution was as follows: 115 mM K-gluconate, 25 mM KCl, 9 mM NaCl, 10 mM HEPES, 0.2 mM EGTA, 1 mM $MgCl_2$, 3 mM K_2-ATP, and 1 mM Na-GTP. The pH and osmolarity (Osm) were adjusted to 7.3 and 280–290 mOsm, respectively.

All signals were grounded using a 3 M KCl-agar bridge electrode (Ag-AgCl wire) and filtered using a low-pass Bessel filter at 2 (voltage-clamp) or 5 (current-clamp) kHz and sampled at 5–10 kHz depending on the experiments. An uncompensated series resistance of <15 MΩ was compensated by 40 %–80 % and monitored periodically during the course of the experiments. Liquid junction potentials between normal bath and pipette solutions were not corrected off-line. After establishment of whole cell configuration, subsequent recordings and analysis were conducted only in the neurons that showed an initial resting potential of ≥−55 mV, an uncompensated Rs of <15 MΩ, and an evoked action potential amplitude of ≥80 mV. Ox-A (Peptide Institute Inc., Osaka, Japan) dissolved in distilled water, sodium channel blocker riluzole (MedChemExpress, NJ, USA) in dimethyl sulfoxide (DMSO), or orexin receptor 1 and 2 antagonist almorexant (MedChemExpress) in DMSO were added to the recording solution. For the isolation of persistent sodium current (I_{NaP}) during voltage clamp recordings, we replaced external solution from normal ACSF with modified ACSF consisting of 131 mM NaCl, 10 mM HEPES, 3 mM KCl, 10 mM glucose, 1 mM $CaCl_2$, 2 mM $MgCl_2$, 10 mM TEA-Cl, 10 mM CsCl, 3 mM 4-AP, and 0.1 mM $CdCl_2$. The specified intrapipette solution contained 130 mM CsF, 9 mM NaCl, 10 mM HEPES, 10 mM EGTA, 1 mM $MgCl_2$, 3 mM K_2-ATP, and 1 mM Na_2-GTP [13].

For frequency-domain analysis, a ZAP input current at frequencies ranging from 0 to 250 Hz was injected into neurons and the membrane voltage responses at resting and subthreshold membrane potentials were recorded. We used a low-pass filter at 0.5 kHz to reduce the noise of the input current. The current and voltage recordings were digitized at a frequency of 10 kHz. The ratio of the fast Fourier transform (FFT) of the voltage response and the input current, calculated using the following formula: Z = FFT (V) / FFT (I), was defined as impedance (Z). The frequency-response curve (FRC) was obtained by plotting the frequency against the magnitude of impedance. The resonant frequency (Fres) was defined as the frequency at the peak of the FRC. The Q-value was calculated by measuring the impedance at Fres and dividing that value by the magnitude of the impedance at the lowest frequency measured [10,11,13].

Numeric results were expressed as means ± standard deviation. Statistical analysis was performed using SPSS version 24.0 (SPSS Inc, Chicago, IL, USA). Depending on the normality of variable distribution and the homogeneity of variances, the comparison of the means of two groups recorded from the same subset of neurons or an independent subset of neurons was analyzed by dependent or independent *t*-test, respectively. In addition, the means of multiple data sets measured from the independent subset or the same subset of neurons under different conditions with normality and homoscedasticity were compared with one-way ANOVA or repeated-measure ANOVA, respectively. A *P* value of <0.05 was considered to indicate statistical significance, unless otherwise stated.

3. Results

The mean values of passive membrane properties for Mes V neurons (total n = 66) were resting membrane potential of −60.9 ± 1.6 mV, input resistance of 86.8 ± 4.4 MΩ, and membrane capacitance of 91.2 ± 8.7 pF, similar to those reported previously [10–13].

3.1. Effects of Ox-A on spike discharge characteristics in Mes V neurons

The action potential characteristics induced by a short (3 ms) depolarizing step current pulse from an adjusted same-holding potential were examined. As shown in Fig.1B, the voltage trajectory before and after application of Ox-A (100 nM) showed no significant changes in the spike height and spike half-amplitude duration; however, Ox-A application induced a modest but significant increase in the medium after-hyperpolarization (mAHP) amplitude (control, −12.6 ± 7.6 mV, Ox-A, −13.4 ± 2.7 mV, $P = 0.032$, dependent *t*-test, n = 20) and a substantial decrease in the half-amplitude duration of after-hyperpolarization (AHP) (control, 61.9 ± 7.6 ms, Ox-A, 33.5 ± 2.7 ms, $P < 0.05$, dependent *t*-test, n = 20) (Fig. 1C).

Repetitive spike discharge induced by long (1 s) step depolarizing pulses could be observed in older (>P6) Mes V neurons [10,11]. Bath application of Ox-A substantially decreased the duration of the train, which could be partially recovered by wash out in 3 out of 6 neurons (Fig. 2A). Additionally, the frequency-time relationship demonstrated that Ox-A hastened the spike frequency adaptation compared to the control condition (Fig. 2B). Both the first interspike interval, ISI (frequency calculated from the interval between the first and the second spikes) and the steady-state frequency (steady-state: the mean value of last five interspike interval frequencies) were significantly increased

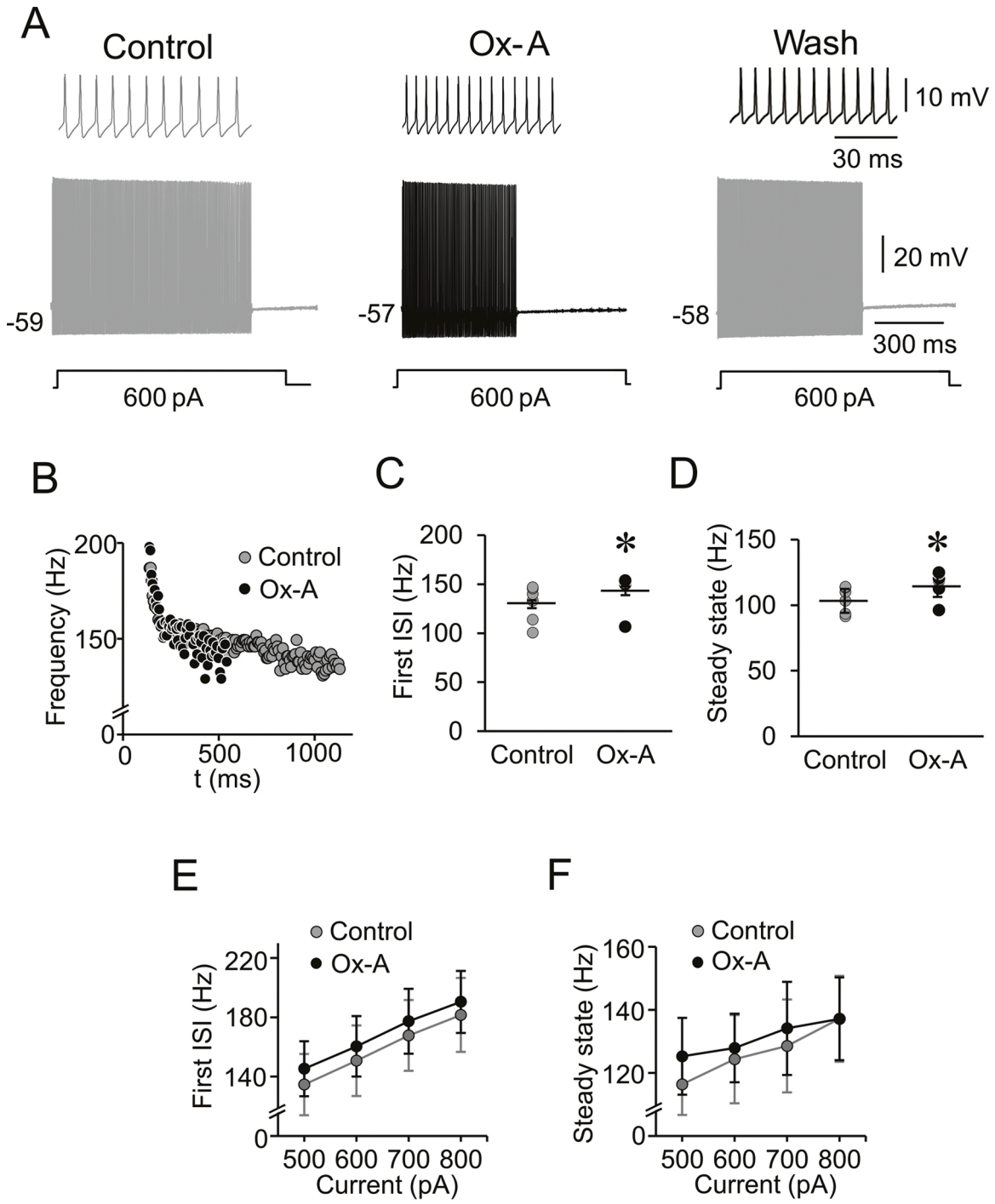

Fig. 2. Effects of Ox-A on spike discharge characteristics in Mes V neurons.
A: Representative examples of repetitive discharge induced by a long (1 s) depolarizing step pulse in P15 neurons before and after application of Ox-A, and after wash out. B: Ox-A application decreased the slope of the frequency-time relationship, and enhanced the spike frequency adaptation. C and D: The mean instantaneous (C) and steady-state (D) spike frequency, measured at 600 pA, were increased by Ox-A application. E and F: The frequency-current relationships for instantaneous (E) and steady-state (F) frequency shifted to the left after application of Ox-A. *$P <$ 0.05.

after Ox-A application (first ISI: control:129.5 ± 7.6 Hz, Ox-A:143.1 ± 7.4 Hz, n = 6, paired *t*-test, $P =$ 0.032, Steady-state: control:103.3 ± 4.0 Hz, Ox-A:115.2 ± 4.4 Hz, n = 6, dependent *t*-test, $P =$ 0.016, induced by current intensity of 600 pA, independent *t*-test, Fig. 2C and D). Likewise, the frequency-current (F–I) relationship revealed that Ox-A showed the trend of increasing the mean first ISI and the steady-state frequency of all trains induced by a series of current stimuli (repeated-measured ANOVA, first ISI: F (1,79) = 1.127, $P =$ 0.302, steady-state: F (1,79) = 0.676, $P =$ 0.422, n =6, Fig. 2E and F).

3.2. *Effects of Ox-A on resonant behavior in Mes V neurons*

Mes V neurons are known to have voltage-dependent resonant behaviors that are mediated by I_{NaP} and h-current (I_h), which are critically involved in the regulation of spike discharge characteristics [10–12]. Therefore, we next examined the effect of Ox-A on the resonant properties. Another subset of neurons held at a voltage slightly depolarized from the resting potential showed a spindle-shaped voltage response by injection of ZAP input current. Application of Ox-A modestly increased

the hump of the impedance-frequency relationship (FRC), which resulted in a significant increase in the Q-value and a small shift in resonant frequency (Q-value: control, 2.7 ± 1.1, Ox-A, 3.3 ± 1.5, dependent *t*-test, $P = 0.037$; Fres: control, 66.7 ± 34.1 Hz, Ox-A, 73.3 ± 33.0 Hz, dependent *t*-test, $P = 0.039$, n = 6, Fig. 3A–C). In contrast, FRC with low peak frequency (<10 Hz) at resting membrane potential showed little change before and after the application of Ox-A, and no significant differences were observed in resonant properties (Q-value: control, 1.6 ± 0.4, Ox-A, 1.6 ± 0.6, dependent *t*-test, $P = 0.391$; Fres: control, 17.6 ± 31.6 Hz, Ox-A, 22.6 ± 38.6 Hz, dependent *t*-test, $P = 0.081$, n = 6, Fig. 3D–F).

3.3. Persistent sodium current participates in Ox-A-mediated modulation in Mes V neurons

Previous studies demonstrated that I_{NaP} is potentially involved in the critical ionic conductance underlying repetitive discharge and subthreshold membrane resonance at depolarization [11,12]. Here, we isolated I_{NaP} using a depolarizing voltage ramp protocol, as confirmed by substantial suppression of the net inward current and peak current density by riluzole (5 μM) (control, 2.77 ± 0.46 pA/pF, riluzole, 0.09 ± 0.10 pA/pF, n = 4, dependent *t*-test, $P = 0.0005$, Fig. 4A), as previously reported [12]. Ox-A increased the peak amplitude, and the peak current density was consistently elevated after Ox-A application (control, 3.24 ± 1.11 pA/pF, Ox-A, 4.20 ± 1.33 pA/pF, n = 5, dependent *t*-test, $P = 0.045$, Fig. 4 B), but this effect was attenuated by the presence of almorexant (1 μM) (control, 2.49 ± 0.57 pA/pF, Ox-A, 2.48 ± 1.07 pA/pF, n = 4, dependent *t*-test, $P = 0.49$, Fig. 4C). In addition, the voltage-dependent activation plots showed a small hyperpolarizing shift of the activation curve ($V_{1/2}$: control, −61.9 ± 2.3 mV, Ox-A, −63.5 ± 2.5 mV, n = 5, dependent *t*-test, $P = 0.001$, Fig. 4D).

4. Discussion

In general, orexinergic neurons are activated by food deprivation as a feeding-promoting peptide and stimulate sensory-motor brainstem regions, including trigeminal neuronal systems, during feeding at both the cellular and behavioral levels [1,8]. In TMNs, Ox-A caused a significant increase in AHP amplitude and lengthened the half-amplitude duration of AHP, whereas only small changes were observed in the spike height or spike half-amplitude duration [9]. Ox-A induced Ca^{2+} influx, thereby elevating intracellular Ca^{2+} levels, which most likely activate Ca^{2+}-dependent K^+ conductance (gK_{Ca}) at rest, leading to amplification of mAHP, which is thought to be involved in the underlying mechanism [9]. In the present study, Ox-A showed little effect on spike height and half-amplitude duration. However, the half-amplitude duration of AHP was significantly decreased with a modest increase in the peak AHP

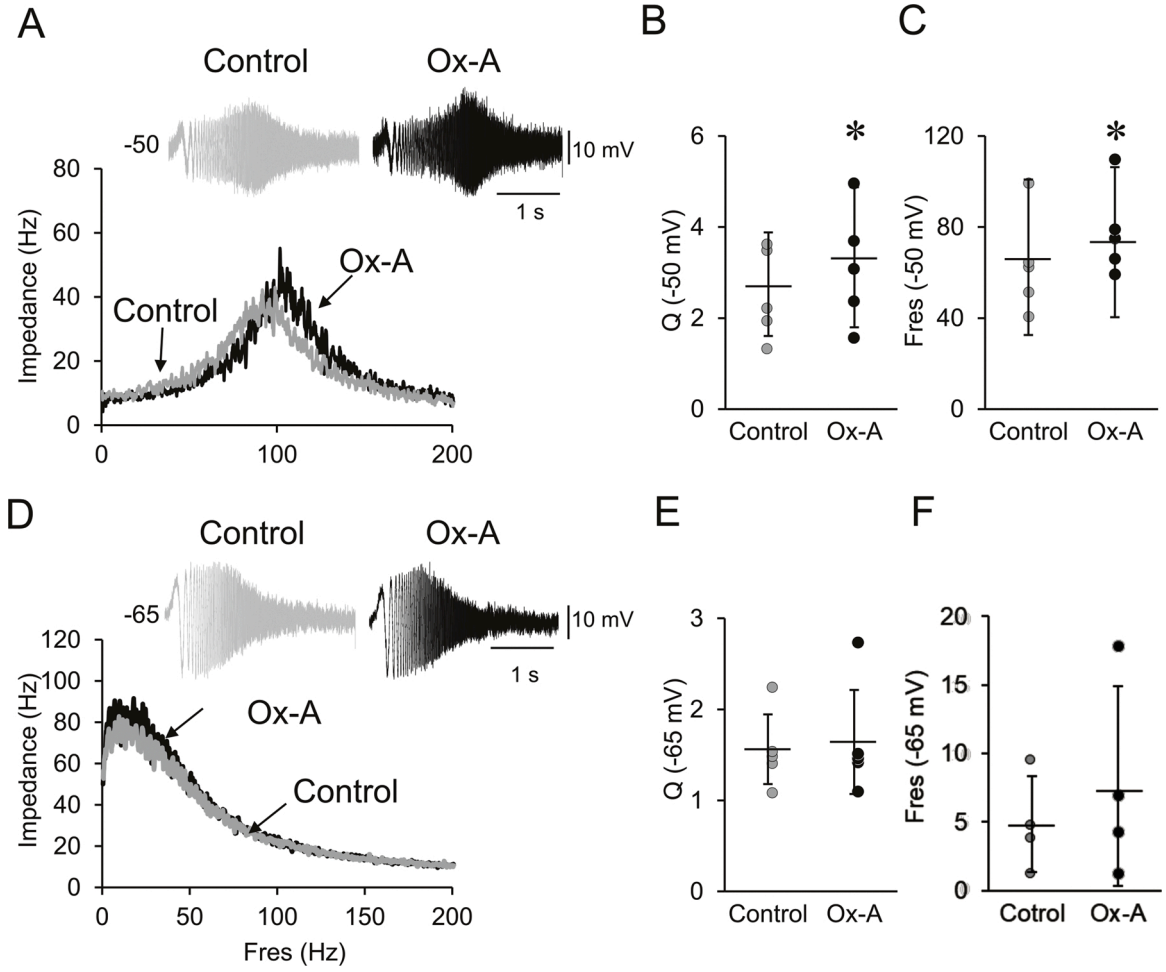

Fig. 3. Effects of Ox-A on resonant behavior in Mes V neurons.
Voltage responses by ZAP current injection at resting and subthreshold membrane potentials before and after application of Ox-A. A–C: Ox-A amplified the voltage response at the subthreshold depolarized membrane potential and increased the peak impedance in the frequency-response curve (A), slightly increasing the Q-value (B) and resonant frequency (C). D-F: At resting membrane potential, Ox-A did not change the frequency-response curve (D), Q-value (E), or resonant frequency (F). *$P < 0.05$.

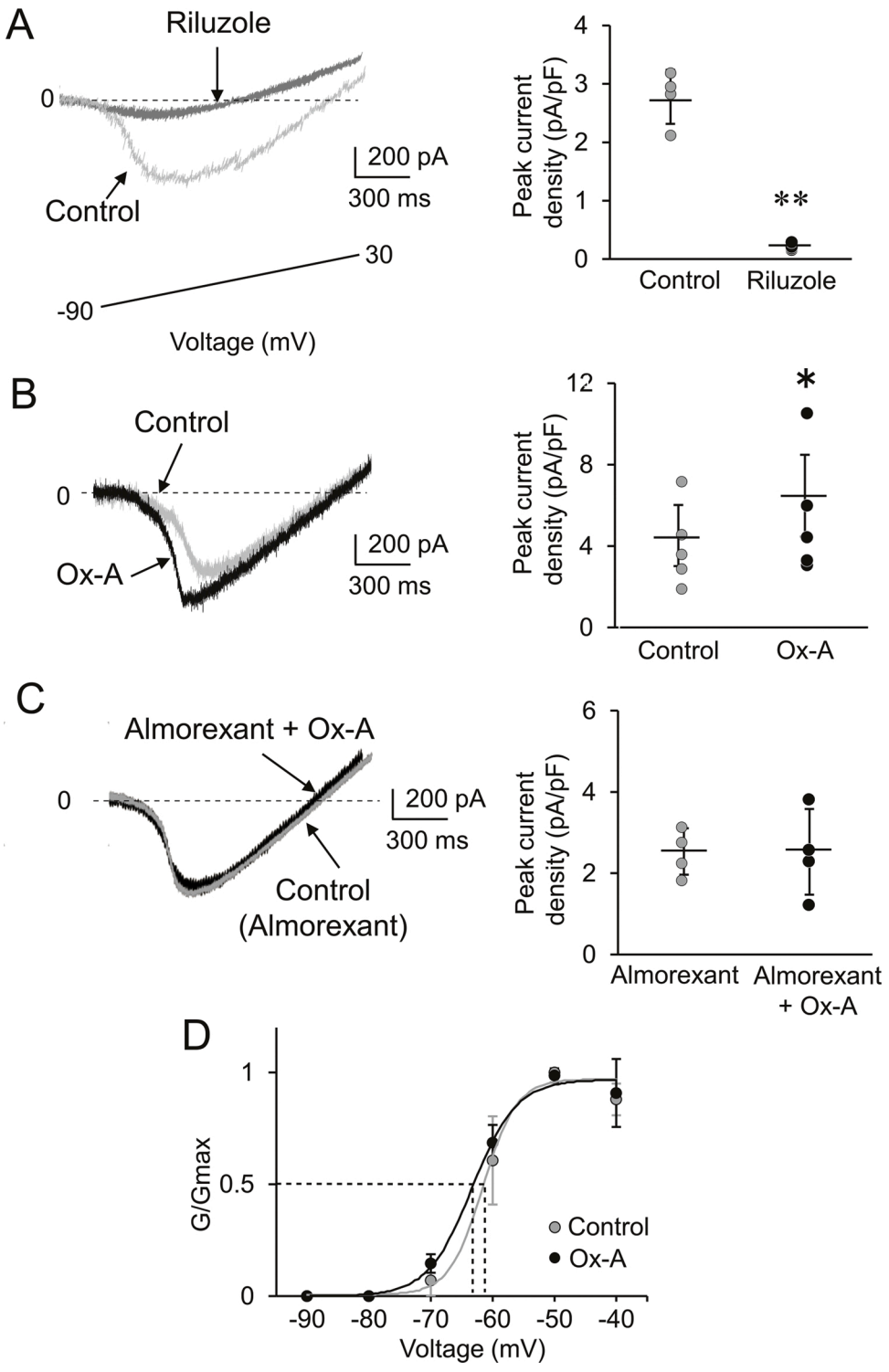

Fig. 4. Ox-A upregulates the persistent sodium current in Mes V neurons.
A and B: Representative current traces induced by a depolarizing voltage ramp protocol from −90 to 30 mV before and after application of riluzole (A) or Ox-A (B) in P15 neurons. Ox-A significantly increased the peak current density of I_{NaP}. C: Pre-treatment with almorexant suppressed the effect of Ox-A. $^{*}P < 0.05$, $^{**}P < 0.01$. D: The I_{NaP} activation curve was fitted with a Boltzmann function, and Ox-A shifted half-maximal activation ($V_{1/2}$) towards hyperpolarization.

amplitude, which resulted in the facilitation of spike repolarization. Consistent with those results, our data showed that Ox-A significantly increased spike frequency during repetitive discharge, with the frequency-current relationship shifted toward hyperpolarization. NPY accelerates the spike repolarization during post-spike AHP in Mes V neurons, and the activation of I_{NaP} is considered to be a powerful candidate because NPY significantly shifts the activation curve of I_{NaP} into the hyperpolarizing direction, which may contribute to an increase in the sustained sodium current upon hyperpolarization and contribute to faster repolarization [13]. Riluzole at concentrations <10 μM suppresses I_{NaP} more than I_{NaT} in Mes V neurons [12], and in the present study 5 μM riluzole substantially attenuated the net inward current induced by voltage ramp in this study, giving us confidence that the net current induced corresponds to I_{NaP}. Ox-A increased the net inward current peak amplitude with an accompanying shift of half-maximal activation towards hyperpolarization, potentially modulating neuronal excitability by the same underlying mechanism as NPY [13].

Supporting these data, Ox-A amplified the resonant Q-value at the subthreshold depolarized membrane potential as previously demonstrated by application of NPY [13]. The subthreshold resonant property

at the depolarized membrane potential is specifically produced by a non-inactivating 4-AP-sensitive K^+ current and the passive resistive and capacitive properties of the membrane, and I_{NaP} contributes to the regulation of the resonance via amplification of the Q-value [11,12].

Meanwhile, Ox-A accelerated spike frequency adaptation and shortened the duration of repetitive spike discharge. Despite only a modest increase in the amplitude of post-spike AHP, most likely resulting from an increase of gK/Ca^{2+}, blockade of the conductance with Cd^{2+} increased burst duration [11,12], and was involved in Ox-A-mediated modulation in Mes V neurons, as previously discussed [13]. Mes V neurons also express inward rectification during membrane hyperpolarization, in which a slow inwardly rectifying conductance, termed I_h, is critically involved [10]. The I_h participates in the regulation of membrane potential and spike repolarization, and in the presence of the specific I_h blocker, ZD7288, spike repolarization during AHP can be delayed [10]. However, in the present study, Ox-A minimally influenced low-frequency resonance at the resting potential produced by I_h conductance, including the Q-value, suggesting no involvement of I_h in Ox-A-mediated modulation of spike discharge characteristics, including AHP.

5. Conclusion

During feeding behavior, various types of orexigenic neuropeptides are believed to interact cooperatively or reciprocally to regulate appetite and behavioral patterns. A previous study demonstrated that the feeding behavior induced by intracerebroventricular administration of orexin-A was partially inhibited by prior administration of an NPY-Y1 receptor-specific antagonist and suggested the possible involvement of the NPY pathway in orexin-A-elicited feeding behavior [16]. Consistent with these data, our results demonstrate that orexin increases Mes V neuronal excitability via amplification of persistent sodium conductance, potentially sharing a common underlying mechanism with another hypothalamic neuropeptide, NPY [13].

Funding

This work was supported by a Grant-in-Aid for Scientific Research(C) (15K11245to S.T.) from the Japan Society for the Promotion of Science.

CRediT authorship contribution statement

Susumu Tanaka: Conceptualization, Formal analysis, Writing - original draft, Writing - review & editing, Funding acquisition. **Soju Seki:** Investigation, Formal analysis, Visualization. **Yudai Ono:** Investigation, Formal analysis. **Akifumi Enomoto:** Formal analysis, Visualization. **Mikihiko Kogo:** Supervision, Project administration.

Declaration of Competing Interest

No conflicts of interest, financial or otherwise, are declared by the authors.

Acknowledgment

None.

References

[1] S. Soya, T. Sakurai, Evolution of orexin neuropeptide system: structure and function, Front. Neurosci. 14 (2020) 691, https://doi.org/10.3389/fnins.2020.00691.
[2] T. Nambu, T. Sakurai, K. Mizukami, Y. Hosoya, M. Yanagisawa, K. Goto, Distribution of orexin neurons in the adult rat brain, Brain Res. 827 (1999) 243–260, https://doi.org/10.1016/s0006-8993(99)01336-0.
[3] S.M. Ahmadi-Soleimani, M. Ghaemi-Jandabi, H. Azizi, S. Semnanian, Orexin type 1 receptor antagonism in lateral paragigantocellularis nucleus attenuates naloxone precipitated morphine withdrawal symptoms in rats, Neurosci. Lett. 558 (2014) 62–66, https://doi.org/10.1016/j.neulet.2013.10.064.
[4] S.M. Ahmadi-Soleimani, V. Mianbandi, H. Azizi, H. Azhdari-Zarmehri, M. Ghaemi-Jandabi, A. Abbasi-Mazar, Y. Mohajer, S.P. Darana, Coregulation of sleep-pain physiological interplay by orexin system: an unprecedented review, Behav. Brain Res. 391 (2020), 112650, https://doi.org/10.1016/j.bbr.2020.112650. Epub 2020 May 24.
[5] J.P. Baird, A. Choe, J.L. Loveland, J. Beck, C.E. Mahoney, J.S. Lord, L.A. Grigg, Orexin-A hyperphagia: hindbrain participation in consummatory feeding responses, Endocrinology 150 (2009) 1202–12016, https://doi.org/10.1210/en.2008-0293.
[6] T. Tsuji, T. Yamamoto, S. Tanaka, S. Bakhshishayan, M. Kogo, Analyses of the facilitatory effect of orexin on eating and masticatory muscle activity in rats, J. Neurophysiol. 106 (2011) 3129–3135, https://doi.org/10.1152/jn.01108.2010.
[7] M.A. Greco, P.J. Shiromani, Hypocretin receptor protein and mRNA expression in the dorsolateral pons of rats, Brain Res. Mol. Brain Res. 88 (2001) 176–182, https://doi.org/10.1016/s0169-328x(01)00039-0.
[8] J.H. Peever, Y.Y. Lai, J.M. Siegel, Excitatory effects of hypocretin-1 (orexin-A) in the trigeminal motor nucleus are reversed by NMDA antagonism, J. Neurophysiol. 89 (2003) 2591–2600, https://doi.org/10.1152/jn.00968.2002.
[9] S. Tanaka, M. Higuchi, S. Seki, A. Enomoto, M. Kogo, Orexins modulate membrane excitability in rat trigeminal motoneurons, J. Oral Sci. 62 (2020) 265–270, https://doi.org/10.2334/josnusd.19-0141.
[10] S. Tanaka, N. Wu, C.F. Hsaio, J. Turman Jr, S.H. Chandler, Development of inward rectification and control of membrane excitability in mesencephalic V neurons, J. Neurophysiol. 89 (2003) 1288–1298, https://doi.org/10.1152/jn.00850.2002.
[11] N. Wu, C.F. Hsiao, S.H. Chandler, Membrane resonance and subthreshold membrane oscillations in mesencephalic V neurons: participants in burst generation, J. Neurosci. 21 (2001) 3729–3739, https://doi.org/10.1523/jneurosci.21-11-03729.2001.
[12] N. Wu, A. Enomoto, S. Tanaka, C.F. Hsiao, D.Q. Nykamp, E. Izhikevich, S. H. Chandler, Persistent sodium currents in mesencephalic v neurons participate in burst generation and control of membrane excitability, J. Neurophysiol. 93 (2005) 2710–2722, https://doi.org/10.1152/jn.00636.2004.
[13] S. Seki, S. Tanaka, S. Yamada, T. Tsuji, A. Enomoto, Y. Ono, S.H. Chandler, M. Kogo, Neuropeptide Y modulates membrane excitability in neonatal rat mesencephalic V neurons, J. Neurosci. Res. 98 (2020) 921–935, https://doi.org/10.1002/jnr.24583.
[14] I.I. Stoyanova, W.L.C. Rutten, J. le Feber, Orexin-A and orexin-B during the postnatal development of the rat brain, Cell. Mol. Neurobiol. 30 (2010) 81–89, https://doi.org/10.1007/s10571-009-9433-z.
[15] P. Trivedi, H. Yu, D.J. MacNeil, L.H. Van der Ploeg, X.M. Guan, Distribution of orexin receptor mRNA in the rat brain, FEBS Lett. 438 (1998) 71–75, https://doi.org/10.1016/s0014-5793(98)01266-6.
[16] Yamanaka, K. Kunii, T. Nambu, N. Tsujino, A. Sakai, I. Matsuzaki, Y. Miwa, K. Goto, T. Sakurai, Orexin-induced food intake involves neuropeptide Y pathway, Brain Res. 859 (2000) 404–409, https://doi.org/10.1016/s0006-8993(00)02043-6.